International Journal of Pharmaceutics 640 (2023) 123001

Contents lists available at ScienceDirect

International Journal of Pharmaceutics

journal homepage: www.elsevier.com/locate/ijpharm

Convolutional neural network-based evaluation of chemical maps obtained by fast Raman imaging for prediction of tablet dissolution profiles

Dorián László Galata [a], Boldizsár Zsiros [a], Gábor Knyihár [b], Orsolya Péterfi [c], Lilla Alexandra Mészáros [a], Ferenc Ronkay [d], Brigitta Nagy [a], Edina Szabó [a], Zsombor Kristóf Nagy [a,*], Attila Farkas [a]

[a] Department of Organic Chemistry and Technology, Faculty of Chemical Technology and Biotechnology, Budapest University of Technology and Economics, Müegyetem rkp. 3., H-1111 Budapest, Hungary
[b] Department of Automation and Applied Informatics, Faculty of Electrical Engineering and Informatics, Budapest University of Technology and Economics, H-1117, Budapest Magyar Tudósok körútja 2 QB-207, Hungary
[c] Department of Drugs Industry and Pharmaceutical Management, University of Medicine, Pharmacy, Sciences and Technology of Târgu Mureș, Gheorghe Marinescu 38, 540139 Târgu Mureș, Romania
[d] Department of Innovative Vehicles and Materials, GAMF Faculty of Engineering and Computer Science, John von Neumann University, 6000 Kecskemét, Hungary

ARTICLE INFO

Keywords:
Fast Raman imaging
Deep learning
Convolutional neural network
Dissolution prediction
Sustained release tablets
Process analytical technology

ABSTRACT

In this work, the capabilities of a state-of-the-art fast Raman imaging apparatus are exploited to gain information about the concentration and particle size of hydroxypropyl methylcellulose (HPMC) in sustained release tablets. The extracted information is utilized to predict the in vitro dissolution profile of the tablets. For the first time, convolutional neural networks (CNNs) are used for the processing of the chemical images of HPMC distribution and to directly predict the dissolution profile based on the image. This new method is compared to wavelet analysis, which gives a quantification of the texture of HPMC distribution, carrying information regarding both concentration and particle size. A total of 112 training and 32 validation tablets were used, when a CNN was used to characterize the particle size of HPMC, the dissolution profile of the validation tablets was predicted with an average f_2 similarity value of 62.95. Direct prediction based on the image had an f_2 value of 54.2, this demonstrates that the CNN is capable of recognizing the patterns in the data on its own. The presented methods can facilitate a better understanding of the manufacturing processes, as detailed information becomes available with fast measurements.

1. Introduction

Vibrational chemical imaging techniques have experienced drastic improvements in the last few years (Hu et al., 2021; Zeng et al., 2022). In former times, acquiring a decently sized chemical image required several hours or even a whole day. Nowadays, however, Raman imaging instruments are more than 1000 times faster than what was available 10 or 15 years ago. For example, when the surface of a solid dosage form, such as a tablet was analyzed with an older apparatus, approximately 1000 spectra could be recorded in 16 h (Galata et al., 2022), while a state-of-the-art fast Raman model can record more than 1 million spectra in 6.5 h (Šašić and Prusnick, 2019). The measurement speed is even more astonishing in the case of near-infrared (NIR) imaging, where Nishii et al. recently demonstrated a system which can analyze up to 4000 tablets per minute (Nishii et al., 2020). These new fast imaging solutions open the possibility of the real-time characterization of several critical vital quality attributes of tablets, as chemical imaging is capable of measuring active pharmaceutical ingredient (API) content (Nishii et al., 2020), particle size (Mészáros et al., 2022), polymorphism (Sarri et al., 2019) or the quality of film coating (Song et al., 2019).

The in vitro dissolution profile is a crucial characteristic of a tablet, as it is meant to represent how the drug is released from the formulation after administration to patients (Zaborenko et al., 2019). This attribute is influenced by the tablet composition, the particle size of the ingredients, and various manufacturing parameters. Currently, in vitro dissolution profiles are routinely measured in appliances built according to the United States Pharmacopoeia (Kuriyama and Ozaki, 2014). However, this technique relies on analyzing a small proportion of the

* Corresponding author.
E-mail address: zsknagy@oct.bme.hu (Z.K. Nagy).

https://doi.org/10.1016/j.ijpharm.2023.123001
Received 6 March 2023; Received in revised form 21 April 2023; Accepted 25 April 2023
Available online 30 April 2023

Table 1
Composition of calibration and validation tablets.

Formulation name	DR content (w/w%)	HPMC content (w/w%)	MCC content (w/w%)	Lactose content (w/w%)	MgSt content (w/w%)	HPMC fraction
Calibration settings						
C01	8	10	20	60	2	<45 μm
C02	8	10	20	60	2	45–63 μm
C03	8	10	20	60	2	63–100 μm
C04	8	10	20	60	2	100–150 μm
C05	8	13.33	20	56.67	2	<45 μm
C06	8	13.33	20	56.67	2	45–63 μm
C07	8	13.33	20	56.67	2	63–100 μm
C08	8	13.33	20	56.67	2	100–150 μm
C09	8	16.66	20	53.34	2	<45 μm
C10	8	16.66	20	53.34	2	45–63 μm
C11	8	16.66	20	53.34	2	63–100 μm
C12	8	16.66	20	53.34	2	100–150 μm
C13	8	20	20	50	2	<45 μm
C14	8	20	20	50	2	45–63 μm
C15	8	20	20	50	2	63–100 μm
C16	8	20	20	50	2	100–150 μm
C17	8	23.33	20	46.67	2	<45 μm
C18	8	23.33	20	46.67	2	45–63 μm
C19	8	23.33	20	46.67	2	63–100 μm
C20	8	23.33	20	46.67	2	100–150 μm
C21	8	26.66	20	43.34	2	<45 μm
C22	8	26.66	20	43.34	2	45–63 μm
C23	8	26.66	20	43.34	2	63–100 μm
C24	8	26.66	20	43.34	2	100–150 μm
C25	8	30	20	40	2	<45 μm
C26	8	30	20	40	2	45–63 μm
C27	8	30	20	40	2	63–100 μm
C28	8	30	20	40	2	100–150 μm
Validation settings						
V01	8	12	20	58	2	<45 μm
V02	8	12	20	58	2	63–100 μm
V03	8	15	20	55	2	45–63 μm
V04	8	15	20	55	2	100–150 μm
V05	8	25	20	45	2	<45 μm
V06	8	25	20	45	2	100–150 μm
V07	8	28	20	42	2	45–63 μm
V08	8	28	20	42	2	63–100 μm

manufactured tablets; it is labor-intensive, time-consuming, requires a large amount of solvents, and it destroys the sample. Therefore, its utilization is not beneficial in a continuous manufacturing environment, where a real-time release testing approach based on Process Analytical Technology (PAT) sensors is more desirable (Markl et al., 2020). This led to the development of multiple strategies to construct surrogate models that predict the dissolution behavior of the product without performing the actual test (Zaborenko et al., 2019). Both first-principles (Horkovics-Kovats et al., 2022) and empirical (Pawar et al., 2016) models have been used to predict the dissolution profile of tablets based on data obtained via PAT sensors. A chemical image carries information about the factors that determine the release rate of the drug, thus, there is a chance of predicting the in vitro dissolution profile of tablets based on chemical images. Yekpe et al. were the first to utilize NIR chemical imaging for that purpose, where the concentration and particle size of the disintegrant determined the drug release rate (Yekpe et al., 2015). More recently, Raman chemical imaging has also been applied in the case of sustained-release tablets where hydroxypropyl methylcellulose is responsible for controlling drug release (Galata et al., 2022; Zeng et al., 2022). These results make it clear that Raman imaging yields an appropriate amount of information for the prediction of the dissolution profile of the tablet. However, in the works presented so far, the time required to acquire a single chemical image is comparable to the length of an actual dissolution run. Therefore, to exploit the true potential of this technique, the application of state-of-the-art fast Raman imaging appliances for this purpose should be tested.

Chemical image processing can be a daunting task as, initially, a large hyperspectral data cube is at hand, where a whole spectrum belongs to each spatial pixel. Firstly, chemometric methods such as Classical Least Squares (CLS) (Vajna et al., 2011) or Multivariate Curve Resolution (MCR) (De Juan et al., 2014) are used to create a distribution map of each component of the analyzed mixture. The obtained concentration maps of the components contain complex information about the sample, which should be further simplified if the goal is to create a regression model based on the map (Galata et al., 2022). Various arbitrary methods can realize the quantitation of the concentration or the particle size of the component. However, in the last decade, unprecedented advances were made in the field of artificial intelligence, leading to the creation of powerful image processing models. The advent of convolutional neural networks (CNNs) (Gu et al., 2018) enabled computers to learn the features of an image robustly and efficiently. CNN-based models have first been used to categorize whole images based on their content (Sharma et al., 2018). However, this technique has since been augmented to recognize individual objects in an image, this has many potential applications in medicine (Li et al., 2019) or the pharmaceutical industry (Ficzere et al., 2022). Using CNNs for regression tasks may be beneficial, thereby quantifying a certain attribute of the image (Zhou et al., 2016). When the unprocessed image is input, the CNN may discover patterns that correlate with the examined quality attribute, which would have been overlooked or lost during feature extraction when arbitrarily chosen algorithms are used. Therefore, CNNs could also be utilized in the analysis of chemical images, both for extracting the relevant features and directly predicting the value of the desired quality attribute.

Consequently, our work has two main goals. Firstly, we intend to create a dataset for predicting the in vitro dissolution profiles of sustained release tablets based on Raman images acquired with a fast imaging apparatus. The applied state-of-the-art imaging device reduces the

map acquisition time to several minutes, making the technique more appealing in industrial R&D and manufacturing quality control. Secondly, we aim to exploit the image processing capability of CNNs for the prediction of the dissolution profile of the tablets. To achieve this, we plan to create dissolution prediction models based on classic image analysis methods and compare them with a CNN-based method. A combination of fast chemical imaging with CNNs can bring vast improvement in quality control by providing a previously unseen quality and quantity of information.

2. Materials and methods

2.1. Materials

The selected model drug, drotaverine hydrochloride (DR) was purchased from Sigma Aldrich (Munich, Germany). The applied matrix polymer, hydroxypropyl methylcellulose (HPMC) K100M DC2 was gifted by Colorcon (Budapest, Hungary). Microcrystalline cellulose (Vivapur 200, MCC) was obtained from JRS Pharma (Rosenberg, Germany). α-lactose monohydrate (Granulac® 70) was supplied by Meggle Pharma (Wasserburg, Germany). Magnesium stearate (MgSt) was chosen as the lubricant, it was purchased from Hungaropharma Ltd. (Budapest, Hungary). Concentrated HCl solution was obtained from Merck (Darmstadt, Germany).

2.2. Methods

2.2.1. Sieving of HPMC

HPMC was separated into four fractions by applying sieves with the following pore sizes: 45 μm, 63 μm, 100 μm and 150 μm. For the sieving, a CISA BA 200 N (Barcelona, Spain) apparatus was used with a vibration amplitude of 2 mm, the procedure was carried out until the mass of the fractions became constant. Fractions with the following particle sizes were collected: <45 μm, 45–63 μm, 63–100 μm, 100–150 μm.

These fractions were characterized using a Malvern Mastersizer 2000 (Malvern, UK) laser diffraction appliance with a Malvern Scirocco 2000 powder feeding inlet. Measurements were carried out with a dispersive air pressure of 2 bar on samples weighing 2 g.

Table 2
Properties of the ANNs used for dissolution prediction. MSE: mean squared error.

Property	WA	WA-CLS	CNN-CLS
Input layer neuron number	2	3	2
Input	scores values from PCA	scores values from PCA + HPMC concentration	particle size from CNN + HPMC concentration
Number of hidden layers	1	1	1
Hidden layer neuron number	1–10 (optimized)	1–10 (optimized)	1–10 (optimized)
Hidden layer transfer function	tangent sigmoid	tangent sigmoid	tangent sigmoid
Output	dissolution profile	dissolution profile	dissolution profile
Output layer neuron number	37	37	37
Output layer transfer function	linear	linear	linear
Training algorithm	Bayesian regularization	Bayesian regularization	Bayesian regularization
Stopping criteria	gradient of MSE performance function < 10^{-7} or epochs > 1000	gradient of MSE performance function < 10^{-7} or epochs > 1000	gradient of MSE performance function < 10^{-7} or epochs > 1000

2.2.2. Preparation of tablets

Tablets were manufactured with a total of 36 compositions (28 for training and 8 for validation). In our earlier works, we found that the concentration and particle size of HPMC are the two most significant factors determining the dissolution rate in tablets of this kind, while the particle size of the drug did not have a strong effect (Galata et al., 2021). Therefore, the two parameters varied between the compositions were the concentration and particle size of HPMC. The actual values for each setting are shown in Table 1. The tablets were compressed on a Dott Bonapace CPR-6 single punch tablet press (Limbiate, Italy) with a force of 15 kN. 14 mm concave punches were utilized, and the target weight of the tablets was 500 mg. 4 tablets were prepared at each composition.

2.2.3. Fast Raman imaging

Raman imaging of the surface of the tablets was performed using a Thermo Scientific DXR3xi (Waltham, Massachussets, USA) apparatus equipped with a 785 nm laser with a power of 30 mW. A microscope objective with a magnification of 20 × was used to acquire the chemical images in line scan mode. An automated sample stage moved the tablet, and an area of 1.2 × 1.2 mm^2 was covered with steps of 40 μm, resulting in the acquisition of 31 columns with 31 spectrum in each column, for a total of 961 spectra. The spectra were recorded with an acquisition time of 0.1 s in the Raman shift region of 200–1800 cm^{-1} and the area was scanned 3 times, this way the total measurement time was 5 min and 48 s for each map.

2.2.4. In vitro dissolution testing

A Hanson SR8-Plus appliance (Chatsworth, CA, USA) was used in USP II configuration (paddle method) to carry out the in vitro dissolution test of the tablets. 900 mL of pH 1.2 HCl solution was used as dissolution medium, the temperature was set to 37 ± 0.5 °C and the rotational speed of the paddles was 100 rpm. The dissolution of the tablets was monitored for 16 h by taking samples at set intervals with a Hanson Autoplus 8 Maximizer (Chatsworth, CA, USA) automatic syringe pump through 10 μm pore size filters. A total of 37 samples were taken at the following time points: 2, 5, 10, 15, 30, 45 and 60 min, after that, every 30 min until 960 min. The DR content in the samples was measured using an Agilent 8453 (Hewlett-Packard, Palo Alto, CA, USA) on-line coupled spectrophotometer by measuring the absorbance at 302 nm in 10 mm flow through cuvettes.

2.3. Data analysis

The calculations described in this chapter were carried out in MATLAB version 9.8 (Mathworks, Natick, MA, USA), utilizing the PLS_Toolbox 8.8.1 (Eigenvector Research, Manson, WA, USA), Wavelet Toolbox 5.4 and Deep Learning Toolbox 14.0.

2.3.1. Data extraction from Raman chemical images

The Classical Least Squares (CLS) method was applied to predict the HPMC content from the Raman spectra at each point of the hyperspectral images, this required the acquisition of the spectra of the pure components. CLS calculates values from 0 to 1 for each component characterizing their concentration in the spectrum. Thus, 31 × 31 chemical maps were obtained for all components. Among the maps, HPMC scores were used to predict the dissolution profile.

Four approaches were used to extract information from the HPMC distribution maps. Wavelet analysis (WA) was applied to a 2D image in the first two cases. It can be used to quantify the texture of the image (Mészáros et al., 2020). As a result, a histogram is obtained, which looks different when the image has a smooth or rough texture. For this analysis, the concentration maps were converted to grayscale images by upscaling the values from 0 to 1 to 0–255. Discrete 2D WA was

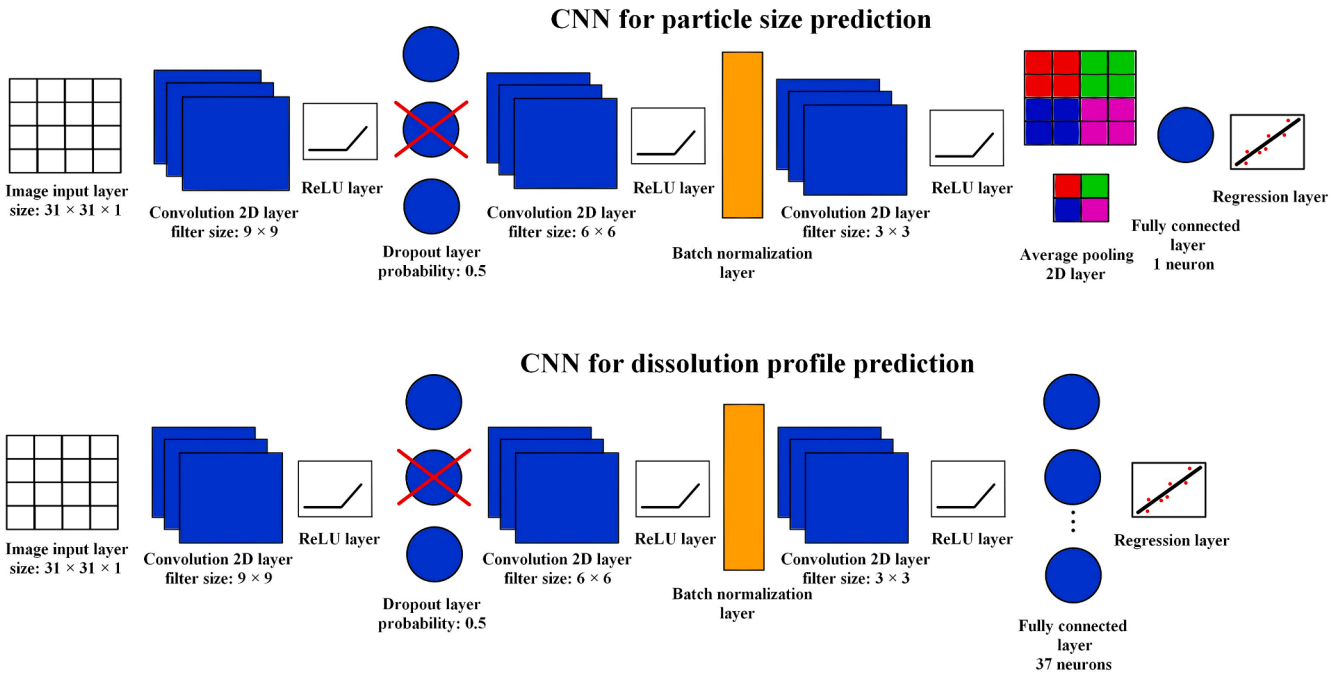

Fig. 1. Architecture of the CNNs used for dissolution and HPMC particle size prediction. ReLU: rectified linear unit.

Table 3
Settings of the CNNs used for dissolution prediction.

Property	HPMC particle size prediction CNN	Dissolution prediction CNN
Training function	Adam	Adam
Validation frequency	5 epochs	5 epochs
Initial learn rate	0.001	0.0005
Learn rate drop period	10 epochs	10 epochs
Learn rate drop factor	0.9	0.95
Maximum epochs	100	200

performed on the images in two steps. Firstly, the image was decomposed using a Daubechies2 wavelet, afterwards, discrete Meyer filters were applied for a second and third decomposition. A histogram was then created from the approximation coefficients, consisting of 600 bins. In order to reduce the dimensionality of the data, the histogram was subjected to Principal Component Analysis (PCA), and the first two score values were retained after this. As preprocessing prior to PCA, Savitzky-Golay smoothing (filter width 15, 2nd order polynomial) and mean centering were applied. In the first approach (WA), these two score values were the input of the dissolution prediction models, while in the second (WA-CLS), this data was augmented with the HPMC concentration of the tablets obtained by averaging the CLS predictions of the 961 spectra.

In the third and fourth scenarios, CNN-based processing was carried out on the chemical maps. The third method is called CNN-CLS, as CNN is applied to characterize the particle size of HPMC, while the HPMC content is obtained by averaging the CLS predictions. In the fourth approach ('only CNN'), the chemical map is the input of a CNN without additional processing and the dissolution profile is predicted directly from the images.

2.3.2. Creation of dissolution prediction models

The four approaches described in the previous chapter require vastly different neural network architectures. In the first three cases, simple feedforward backpropagation ANNs were used for the prediction of the dissolution profiles, their properties are summarized in Table 2. The 112 (28 × 4) training samples were split randomly into the following categories: training (70%), cross-validation (15%) and testing (15%).

In the 'only CNN' and CNN-CLS approaches, CNNs were applied for two different purposes. In the CNN-CLS method, a CNN was trained to predict the particle size of HPMC based on the chemical maps of the 112 training tablets. The size of the smallest sieve through which the fraction has passed was chosen to be the output of this CNN. The constructed model was then used to predict the HPMC fraction of the tablets which was used as input in a feedforward backpropagation ANN. In the 'only CNN' approach, the CNN used the chemical maps as input to directly predict the dissolution profile of the tablets. The architecture and parameters of the models are shown in Fig. 1 and Table 3, respectively.

The neuron number of the ANNs in the hidden layer was optimized with numbers between 1 and 10. The dissolution prediction CNN gave variable results after multiple runs, therefore it was run 100 times to choose the best-performing model. The predictive ability of the models was evaluated using the f_2 similarity factor (Equation (1)), which has values between 0 and 100. The more similar the predicted and measured dissolution profiles, the higher the value:

$$f_2 = 50log_{10}\left\{\left[1+\frac{1}{n}\sum_{i=1}^{n} w_t(R_t - T_t)^2\right]^{0.5} *100\right\} \quad (1)$$

where R_t and T_t refer to the dissolution values measured and predicted at time point t, respectively, w_t is an optional weighing factor and n is the number of measurement points in the dissolution curve. The parameter is applied in a way that only points before 85% dissolution are used and one point after 85%, this way, the easily predicted flat end of the curve is not taken into consideration (Duan et al., 2011).

3. Results and discussion

3.1. Information extraction from the Raman chemical images

In order to characterize the HPMC concentration and particle size of the tablets, the Raman chemical images were processed using the CLS method to obtain the concentration map of HPMC. Based on a visual

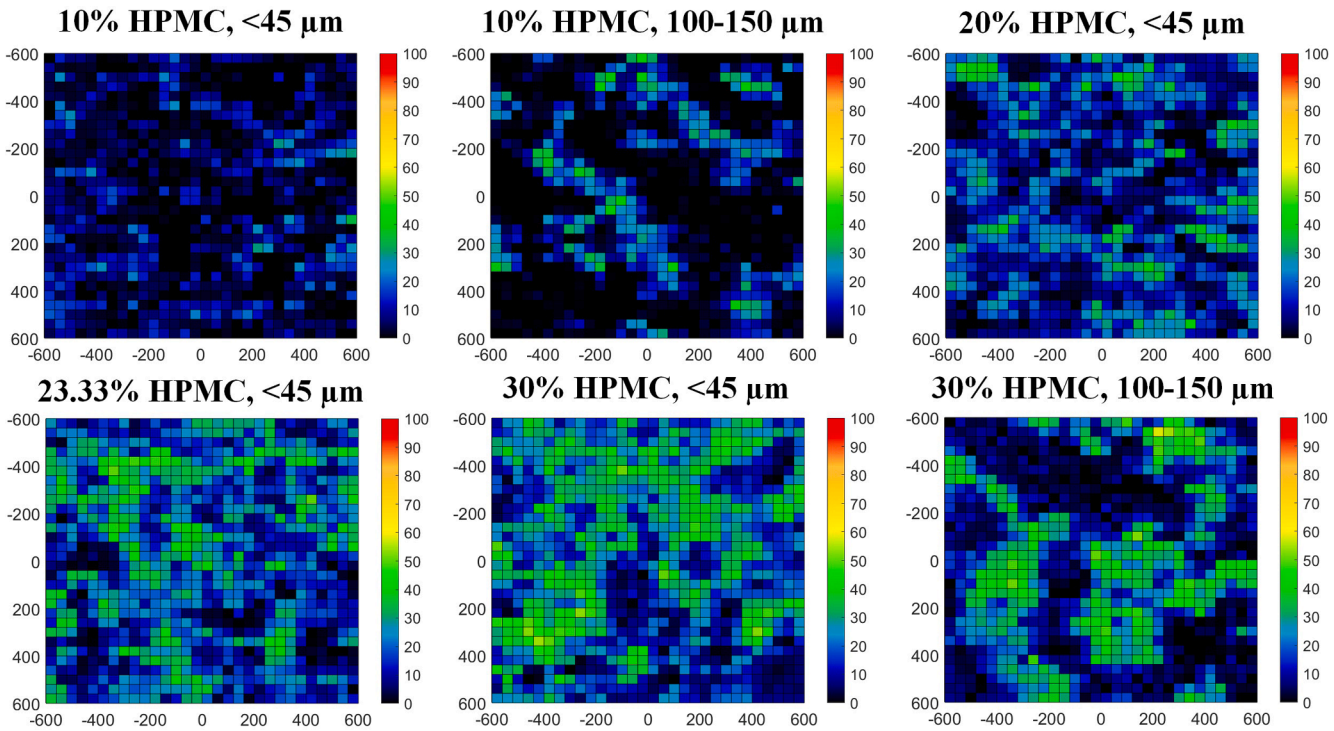

Fig. 2. Examples of chemical maps of tablets with various HPMC concentrations and particle sizes. The colorbars on the right represent the concentration of HPMC predicted by the CLS method. The numbers on the left and bottom represent distance measured in micrometers.

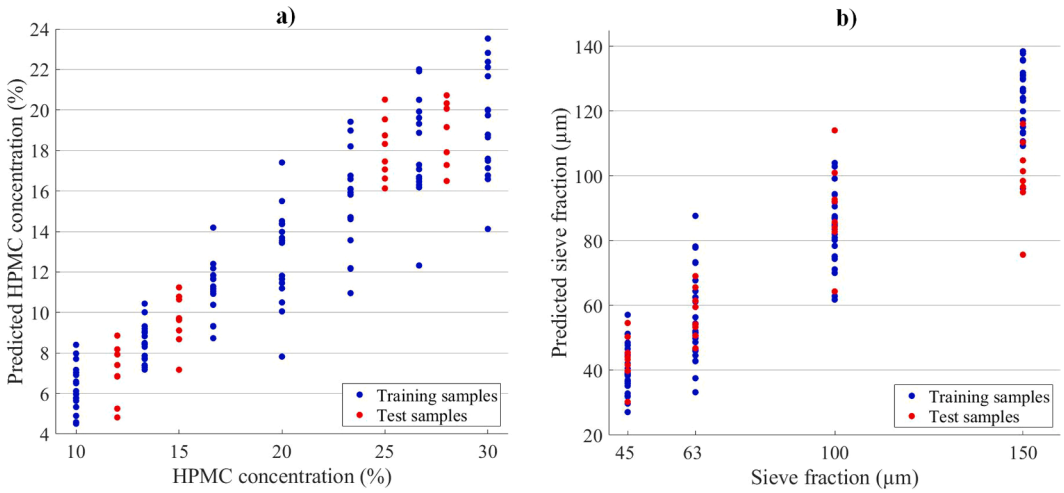

Fig. 3. A) hpmc concentration of tablets values predicted by the cls method. b) hpmc sieve fraction of tablets predicted with cnn.

inspection, these images can be used to differentiate various concentrations and particle size fractions (Fig. 2). As the concentration increases, more pixels with high HPMC content can be observed. When the particle size is larger, high intensity pixels are clustered and there are regions lacking HPMC between them, while the distribution is more uniform with smaller particle sizes. Unlike in our previous work (Galata et al., 2022), this time, the tablets contain both HPMC and MCC. These have a very similar composition, therefore the applied spectroscopic technique must have a strong sensitivity to minor differences in order to make them distinguishable in the chemical image.

The predicted HPMC concentration values were averaged for the whole map to obtain a single value representing the whole tablet, the results of this operation are shown in Fig. 3a. It can be seen that the predicted values have a constant bias, this can be attributed to the fact that the Raman signal of HPMC is not very intense compared to drotaverine and lactose, therefore the CLS method, due to intensity normalization, predicts a lower contribution to the spectrum. However, despite this, the predicted concentrations follow the trend of the real composition of the tablets.

The CNN trained for predicting the HPMC sieve fraction of the tablets is also promising, as seen in Fig. 3b. The model can effectively differentiate between the smaller fractions, the predictions are less satisfying only in the case of the test tablets with the 100–150 µm HPMC fraction.

The score values of the first two principal components (PCs) obtained from the PCA of the wavelet histograms are shown in Fig. 4. Both values show a correlation with the concentration and particle size of HPMC, however, the two effects cannot be clearly separated. The values of the first PC become smaller as HPMC concentration increases, and at one concentration level, higher particle sizes have higher values. At small concentrations, the second PC shows a stronger correlation with particle

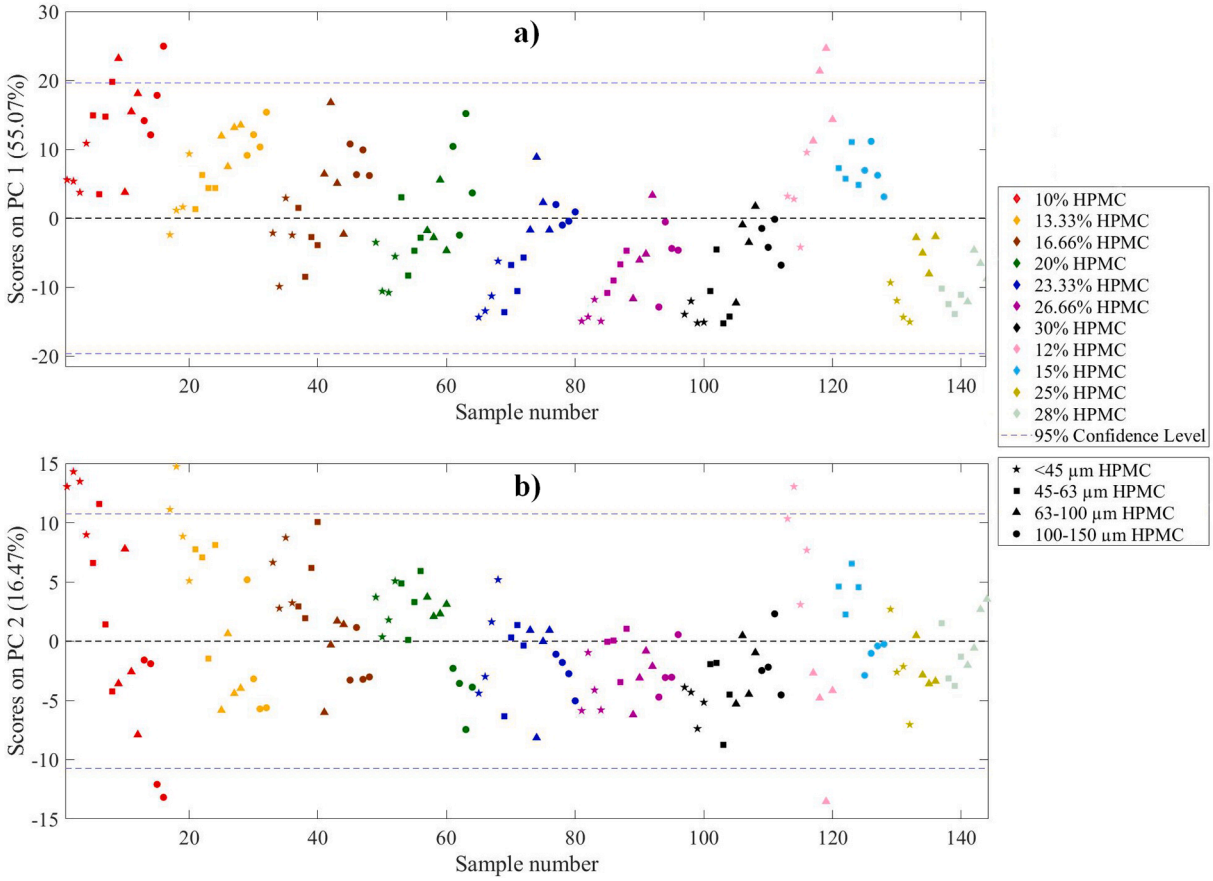

Fig. 4. A) score values on the first pc of the wavelet histograms. b) score values on the second pc of the wavelet histograms. the color of the markers indicates hpmc content, while the marker shape refers to hpmc particle size.

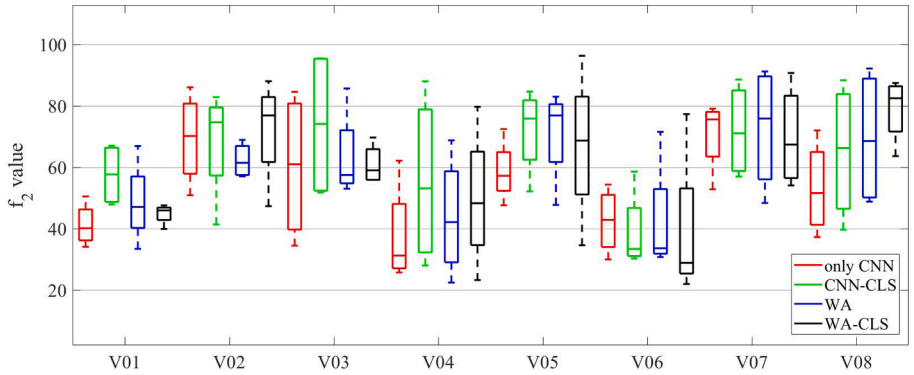

Fig. 5. F_2 value of the predictions obtained for the 8 validation formulations using the 4 different methods. The central line of the boxes mark the median, the bottom and top edges refer to the 25th and 75th percentiles, respectively, the whiskers extend to cover the most extreme data points which are not outliers.

size, however, this diminishes when the concentration is higher than 20%.

The success of data extraction shown in Figs. 2-4 implies that Raman chemical imaging is capable of differentiation between HPMC and MCC, as both the concentration and particle size of HPMC could be effectively characterized.

3.2. Prediction of dissolution profiles

After the necessary data extraction was performed, ANN and CNN models were created to predict the dissolution profile of the tablets. The f_2 value of the obtained predictions is shown in Fig. 5.

The average f_2 value and the optimal neuron number in the hidden layer of the four methods is listed in Table 4. A small number of hidden neurons is sufficient for modeling the effect of the varied parameters on the dissolution curve. The CNN-CLS method generally yields the best

Table 4
Optimal neuron number in the hidden layer and average f_2 value of the predictions with the four methods.

Method	Number of neurons in hidden layer	Average f_2
Only CNN	–	54.20
CNN-CLS	3	62.95
WA	2	59.26
WA-CLS	4	60.41

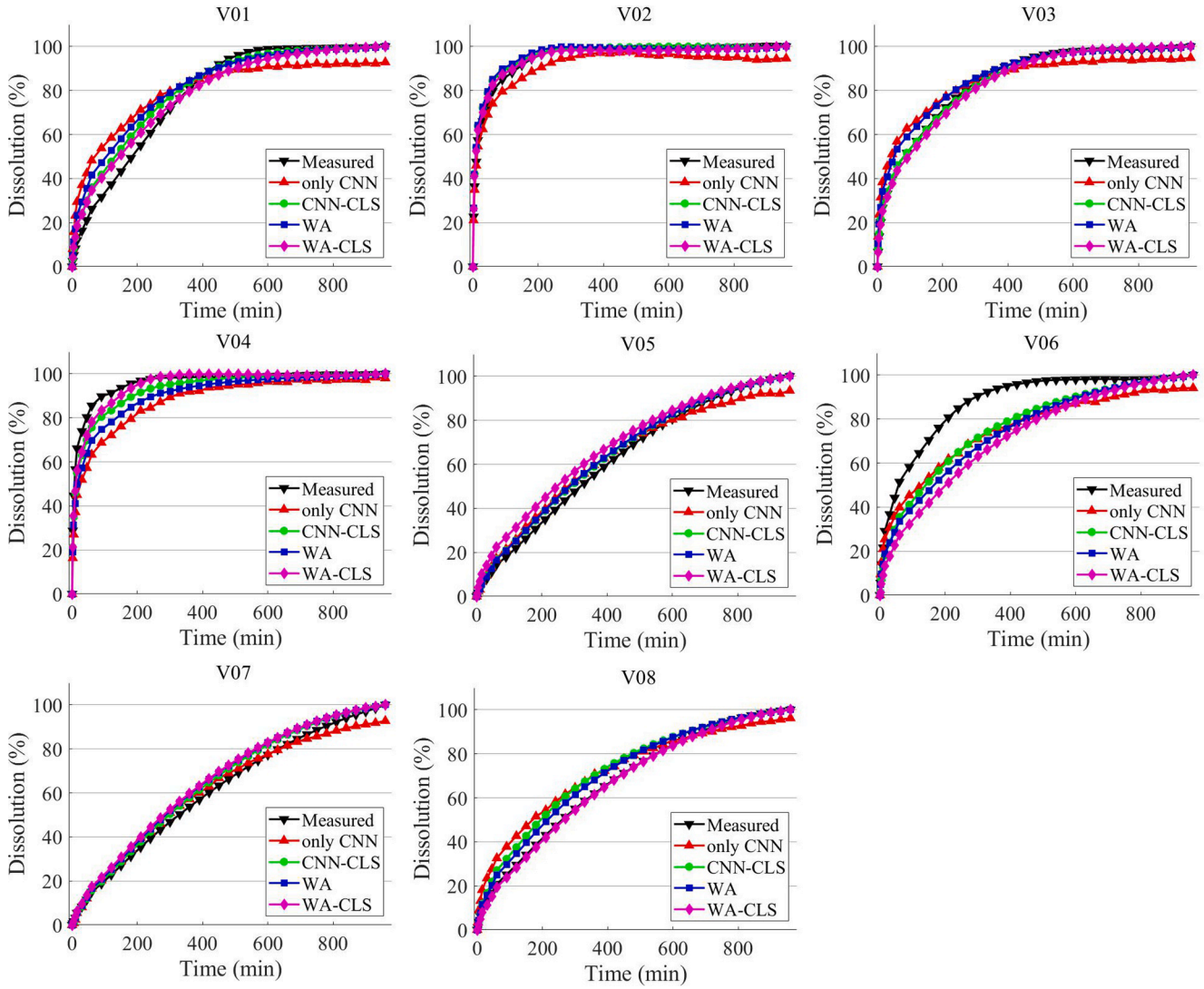

Fig. 6. Average measured and predicted dissolution profiles of the 8 validation formulations.

predictions, while WA and WA-CLS are slightly less accurate. It is remarkable that the 'only CNN' method, predicting the profiles directly from the chemical images, also yields good results.

Fig. 6 shows the average predictions obtained for the 8 validation formulations. All four methods apparently give a satisfying prediction of the measured dissolution curve, the 'only CNN' method has lower f_2 values because its predictions are a bit farther from the real dissolution. Nonetheless, it is capable of recognizing the working principles of the tablets similarly to the other three methods utilizing additional processing. The two formulations with the least accurate predictions are V04 and V06. These both have the 100–150 μm HPMC fraction. In both cases, the predicted dissolution is slower than the measured. This observation can be explained by the fact that when the particle size of HPMC is too large, its measurement based on the chemical maps becomes less reliable. This appears in Fig. 3b, where the predicted particle size of the two 100–150 μm validation formulations is smaller than it should be. This phenomenon does not occur with smaller particle sizes. Presumably, a larger area would be desirable to map for reliable measurement of particles bigger than 100 μm, thus, the issues experienced here can be prevented.

4. Conclusions

Overall, fast Raman imaging was proven to be an excellent information source for the dissolution prediction of sustained release tablets. If the current rate of progress in instrument development can be maintained, real-time applications of the technology might become available in a few years. This progression will revolutionize quality assurance of pharmaceutical products, as both the quantity and particle size of components will be measurable in all the produced tablets. Manufacturers will be able to identify and remove individual faulty tablets without compromising the whole batch, while trends in the process, such as a particle size shift due to segregation, will also be easier to recognize.

With the development of CNNs, information extraction from the chemical maps will become more effective, as the direct prediction of the dissolution profile from the map demonstrated here does not require preprocessing steps during which valuable information might be lost. CNNs were shown here to be capable of predicting the dissolution profile on their own, while they are also excellent for data extraction purposes.

CRediT authorship contribution statement

Dorián László Galata: Writing – original draft, Methodology. **Boldizsár Zsiros:** Investigation, Visualization. **Gábor Knyihár:** Investigation. **Orsolya Péterfi:** Investigation. **Lilla Alexandra Mészáros:** Data curation, Software. **Ferenc Ronkay:** Methodology, Writing – review & editing. **Brigitta Nagy:** Writing – review & editing. **Edina**

Szabó: Writing – review & editing. **Zsombor Kristóf Nagy:** Conceptualization, Writing – review & editing. **Attila Farkas:** Supervision.

Declaration of Competing Interest

The authors declare that they have no known competing financial interests or personal relationships that could have appeared to influence the work reported in this paper.

Data availability

Data will be made available on request.

Acknowledgment

This work was supported by OTKA grants K-143039 and PD-142970. Project no. 2019-1.3.1-KK-2019-00004 has been implemented with the support provided from the National Research, Development and Innovation Fund of Hungary, financed under the 2019-1.3.1-KK funding scheme. This work was supported by the ÚNKP-22-4-II-BME-137 New National Excellence Program of the Ministry for Innovation and Technology from the source of the National Research, Development and Innovation Fund. This paper was supported by the János Bolyai Research Scholarship of the Hungarian Academy of Science.

References

De Juan, A., Jaumot, J., Tauler, R., 2014. Multivariate Curve Resolution (MCR). Solving the mixture analysis problem. Anal. Methods 6 (14), 4964–4976.

Duan, J.Z., Riviere, K., Marroum, P., 2011. In vivo bioequivalence and in vitro similarity factor (f2) for dissolution profile comparisons of extended release formulations: how and when do they match? Pharm. Res. 28 (5), 1144–1156.

Ficzere, M., Mészáros, L.A., Kállai-Szabó, N., Kovács, A., Antal, I., Nagy, Z.K., Galata, D. L., 2022. Real-time coating thickness measurement and defect recognition of film coated tablets with machine vision and deep learning. Int. J. Pharm. 623, 121957.

Galata, D.L., Könyves, Z., Nagy, B., Novák, M., Mészáros, L.A., Szabó, E., Farkas, A., Marosi, G., Nagy, Z.K., 2021. Real-time release testing of dissolution based on surrogate models developed by machine learning algorithms using NIR spectra, compression force and particle size distribution as input data. Int. J. Pharm. 597, 120338.

Galata, D.L., Zsiros, B., Mészáros, L.A., Nagy, B., Szabó, E., Farkas, A., Nagy, Z.K., 2022. Raman mapping-based non-destructive dissolution prediction of sustained-release tablets. J. Pharm. Biomed. Anal. 212, 114661.

Gu, J., Wang, Z., Kuen, J., Ma, L., Shahroudy, A., Shuai, B., Liu, T., Wang, X., Wang, G., Cai, J., Chen, T., 2018. Recent advances in convolutional neural networks. Pattern Recogn. 77, 354–377.

Horkovics-Kovats, S., Galata, D.L., Zlatoš, P., Nagy, B., Mészáros, L.A., Nagy, Z.K., 2022. Raman-based real-time dissolution prediction using a deterministic permeation model. Int. J. Pharm. 617, 121624.

Hu, C., Wang, X., Liu, L., Fu, C., Chu, K., Smith, Z.J., 2021. Fast confocal Raman imaging via context-aware compressive sensing. Analyst 146 (7), 2348–2357.

Kuriyama, A., Ozaki, Y., 2014. Assessment of active pharmaceutical ingredient particle size in tablets by Raman chemical imaging validated using polystyrene microsphere size standards. AAPS PharmSciTech 15 (2), 375–387.

Li, Z., Dong, M., Wen, S., Hu, X., Zhou, P., Zeng, Z., 2019. CLU-CNNs: Object detection for medical images. Neurocomputing 350, 53–59.

Markl, D., Warman, M., Dumarey, M., Bergman, E.-L., Folestad, S., Shi, Z., Manley, L.F., Goodwin, D.J., Zeitler, J.A., 2020. Review of real-time release testing of pharmaceutical tablets: State-of-the art, challenges and future perspective. Int. J. Pharm. 582, 119353.

Mészáros, L.A., Galata, D.L., Madarász, L., Köte, Á., Csorba, K., Dávid, Á.Z., Domokos, A., Szabó, E., Nagy, B., Marosi, G., Farkas, A., Nagy, Z.K., 2020. Digital UV/VIS imaging: A rapid PAT tool for crushing strength, drug content and particle size distribution determination in tablets. Int. J. Pharm. 578, 119174.

Mészáros, L.A., Farkas, A., Madarász, L., Bicsár, R., Galata, D.L., Nagy, B., Nagy, Z.K., 2022. UV/VIS imaging-based PAT tool for drug particle size inspection in intact tablets supported by pattern recognition neural networks. Int. J. Pharm. 620, 121773.

Nishii, T., Matsuzaki, K., Morita, S., 2020. Real-time determination and visualization of two independent quantities during a manufacturing process of pharmaceutical tablets by near-infrared hyperspectral imaging combined with multivariate analysis. Int. J. Pharm. 590, 119871.

Pawar, P., Wang, Y., Keyvan, G., Callegari, G., Cuitino, A., Muzzio, F., 2016. Enabling real time release testing by NIR prediction of dissolution of tablets made by continuous direct compression (CDC). Int. J. Pharm. 512 (1), 96–107.

Sarri, B., Canonge, R., Audier, X., Lavastre, V., Pénarier, G., Alie, J., Rigneault, H., 2019. Discriminating polymorph distributions in pharmaceutical tablets using stimulated Raman scattering microscopy. J. Raman Spectrosc. 50 (12), 1896–1904.

Šašić, S., Prusnick, T., 2019. Fast Raman chemical imaging of tablets with non-flat surfaces. Int. J. Pharm. 565, 143–150.

Sharma, N., Jain, V., Mishra, A., 2018. An analysis of convolutional neural networks for image classification. Procedia Comput. Sci. 132, 377–384.

Song, S.W., Kim, J., Eum, C., Cho, Y., Park, C.R., Woo, Y.-A., Kim, H.M., Chung, H., 2019. Hyperspectral Raman line mapping as an effective tool to monitor the coating thickness of pharmaceutical tablets. Anal. Chem. 91 (9), 5810–5816.

Vajna, B., Patyi, G., Nagy, Z., Bódis, A., Farkas, A., Marosi, G., 2011. Comparison of chemometric methods in the analysis of pharmaceuticals with hyperspectral Raman imaging. J. Raman Spectrosc. 42 (11), 1977–1986.

Yekpe, K., Abatzoglou, N., Bataille, B., Gosselin, R., Sharkawi, T., Simard, J.-S., Cournoyer, A., 2015. Predicting the dissolution behavior of pharmaceutical tablets with NIR chemical imaging. Int. J. Pharm. 486 (1–2), 242–251.

Zaborenko, N., Shi, Z., Corredor, C.C., Smith-Goettler, B.M., Zhang, L., Hermans, A., Neu, C.M., Alam, M.A., Cohen, M.J., Lu, X., Xiong, L., Zacour, B.M., 2019. First-principles and empirical approaches to predicting in vitro dissolution for pharmaceutical formulation and process development and for product release testing. AAPS J. 21 (3), 1–20.

Zeng, Q., Wang, L., Wu, S., Fang, G., Zhao, M., Li, Z., Li, W., 2022. Research Progress on the Application of Spectral Imaging Technology in Pharmaceutical Tablet Analysis. Int. J. Pharm. 625, 122100.

Zeng, Q., Wang, L., Wu, S., Fang, G., Liu, H., Li, Z., Hu, Y., Li, W., 2022. Dissolution profiles prediction of sinomenine hydrochloride sustained-release tablets using Raman mapping technique. Int. J. Pharm. 620, 121743.

Zhou, J., Hong, X., Su, F., Zhao, G., 2016. Recurrent convolutional neural network regression for continuous pain intensity estimation in video. *Proceedings of the IEEE Conference on Computer Vision and Pattern Recognition Workshops*.